

Global Analysis of Helicity Parton Densities and Their Uncertainties

Daniel de Florian and Rodolfo Sassot

*Departamento de Física, Universidad de Buenos Aires,
Ciudad Universitaria, Pabellon 1 (1428) Buenos Aires, Argentina*

Marco Stratmann

Radiation Laboratory, RIKEN, 2-1 Hirosawa, Wako, Saitama 351-0198, Japan

Werner Vogelsang

Physics Department, Brookhaven National Laboratory, Upton, NY 11973

We present a new analysis of the helicity parton distributions of the nucleon. The analysis takes into account the available data from inclusive and semi-inclusive polarized deep inelastic scattering, as well as from polarized pp scattering at RHIC. For the first time, all theoretical calculations are performed fully at next-to-leading order (NLO) of perturbative QCD, using a method that allows to incorporate the NLO corrections in a very fast and efficient way in the analysis. We find evidence for a rather small gluon polarization in the nucleon, over a limited region of momentum fraction, and for interesting flavor patterns in the polarized sea.

PACS numbers: 13.88.+e, 12.38.Bx, 13.60.Hb, 13.85.Ni

Introduction.—The exploration of the inner structure of the nucleon is of fundamental importance in Nuclear and Particle Physics. Of particular interest is the spin structure of the nucleon, which addresses questions such as how the nucleon spin is composed of the spins and orbital angular momenta of the quark and gluons inside the nucleon. In deep inelastic scattering (DIS) of leptons off polarized nucleons it was found that surprisingly little of the proton spin is carried by the quark and antiquark spins [1]. This has triggered much theoretical progress, and led to new experiments dedicated to unraveling the proton spin structure. Among them, experiments in polarized proton-proton collisions at the BNL Relativistic Heavy Ion Collider, RHIC, have recently opened a new stage in this quest.

The structure of a nucleon in a helicity eigenstate is foremost described by the (anti)quark and gluon helicity parton distribution functions (PDFs), defined by

$$\Delta f_j(x, Q^2) \equiv f_j^+(x, Q^2) - f_j^-(x, Q^2). \quad (1)$$

Here, $f_j^+(x, Q^2)$ [$f_j^-(x, Q^2)$] denotes the distribution of a parton of type j with positive [negative] helicity in a nucleon with positive helicity, having light-cone momentum fraction x of the nucleon momentum and being probed at a hard scale Q . The integral $\Delta f_j^1(Q^2) \equiv \int_0^1 \Delta f_j(x, Q^2) dx$ measures the spin contribution of parton j to the proton spin, which is one reason why there are world-wide efforts to extract the $\Delta f_j(x, Q^2)$ from experimental data.

The non-perturbative but universal Δf_j are accessible in measurements of double-spin asymmetries,

$$A_{LL} \equiv \frac{d\Delta\sigma}{d\sigma} \equiv \frac{d\sigma^{++} - d\sigma^{+-}}{d\sigma^{++} + d\sigma^{+-}}, \quad (2)$$

for processes characterized by large momentum transfer and helicity settings \pm . Taking high transverse momen-

tum (p_T) reactions in polarized pp scattering as an example, the cross section at hadron-level schematically reads up to corrections suppressed by inverse powers of p_T :

$$d\Delta\sigma = \sum_{ab} \int dx_a \int dx_b \Delta f_a(x_a, Q^2) \Delta f_b(x_b, Q^2) \times d\Delta\hat{\sigma}_{ab}(x_a, x_b, p_T, \alpha_s(Q^2), p_T/Q). \quad (3)$$

The sum runs over all initial partons a, b , with $d\Delta\hat{\sigma}_{ab}$ the corresponding partonic cross sections, defined in analogy with Eq. (2). We note that depending on the experimental observable, also an additional fragmentation function may occur in Eq. (3). An equation similar to (3) holds for the unpolarized cross section $d\sigma$. The $d\Delta\hat{\sigma}_{ab}$ depend only on scales of the order of the hard scale p_T and are hence amenable to QCD perturbation theory. A consistent NLO analysis of (3) requires use of NLO partonic cross sections and scale evolution for the PDFs.

In DIS, an expression analogous to the one in Eq. (3) holds, except that there is only one parton distribution. Efforts over the past three decades have produced extensive data sets for polarized DIS [2]. Results from semi-inclusive DIS (SIDIS) [2, 3], $lN \rightarrow lhX$, with h an identified hadron in the final state, have the promise to put individual constraints on the various quark flavor distributions in the nucleon. Recently, the first precise (in part still preliminary) A_{LL} measurements from RHIC have emerged [4], which are expected to put significant constraints on the helicity gluon distribution, $\Delta g(x, Q^2)$, along with results from lepton nucleon scattering [5].

This paper presents the first “global” NLO analysis of the data from DIS, SIDIS, and RHIC in terms of the helicity PDFs. While there have been quite a few NLO analyses of the polarized DIS data in the past (see, e.g., Refs. [6, 7, 8]), some of which [8] also take into account in-

formation from SIDIS, the full inclusion of RHIC data in the NLO analysis is a new feature. The fact that the cross section in the pp case, Eq. (3), is bilinear in the PDFs, its more complicated kinematic structure, and the overall high complexity of NLO partonic cross sections, present significant technical challenges in this endeavor. Based on a technique presented in [9], we have now developed and commissioned a systematic procedure for performing full NLO analyses also when using pp scattering data.

Global analysis and Mellin technique.—The idea behind a global analysis is to extract the universal PDFs entering factorized cross sections such as Eq. (3) by optimizing the agreement between the measured spin asymmetries for DIS, SIDIS, and pp scattering, relative to the accuracy of the data, and corresponding theoretical calculations, through variation of the shapes of the polarized PDFs. To be specific, we choose an initial scale for the evolution of $Q_0 = 1$ GeV and assume the helicity PDFs to have the following flexible functional forms:

$$x\Delta f_j(x, Q_0^2) = N_j x^{\alpha_j} (1-x)^{\beta_j} (1 + \gamma_j \sqrt{x} + \eta_j x), \quad (4)$$

with free parameters $N_j, \alpha_j, \beta_j, \gamma_j, \eta_j$. The strategy is, then, to evolve the distributions at NLO to the scales relevant to the various data points, to use the evolved distributions to calculate the NLO theoretical spin asymmetries at the kinematics of each data point, and to construct a χ^2 function testing the goodness of fit. The optimal parameters are then found by minimizing χ^2 .

The main technical challenge in our analysis lies in the inclusion of the RHIC A_{LL} data. The χ^2 minimization procedure easily requires of the order of 10^5 or more evaluations of the rather complex NLO pp cross sections [10] for each data point, so that the computer time needed for a minimization directly on the basis of Eq. (3) becomes excessive. In Ref. [9], we devised a method that allows to overcome this problem by working in Mellin-moment space. This is the approach that we will also pursue here.

In short, it amounts to expressing the PDFs in Eq. (3) by their Mellin inverse transformations to find,

$$\begin{aligned} d\Delta\sigma &= -\frac{1}{4\pi^2} \sum_{ab} \int_{\mathcal{C}_n} dn \int_{\mathcal{C}_m} dm \Delta f_a^n(Q^2) \Delta f_b^m(Q^2) \\ &\times \int dx_a \int dx_b x_a^{-n} x_b^{-m} d\Delta\hat{\sigma}_{ab}(x_a, x_b, \dots), \end{aligned} \quad (5)$$

where $\mathcal{C}_{n,m}$ denote appropriate integration contours in complex n, m -space, see [9] for details. Here, the crucial point is that the information on the PDFs, contained in the Mellin moments Δf_a^n and Δf_b^m , defined as usual by $\Delta f_j^n(Q^2) \equiv \int_0^1 dx x^{n-1} \Delta f_j(x, Q^2)$, has been separated from the numerically tedious and time consuming part involving the $d\Delta\hat{\sigma}_{ab}$ in the second row of Eq. (5). As the latter do not depend on the PDFs, their values can be computed prior to the fitting procedure, on a suitable array of moments n and m . Once this has been done,

the remaining inverse Mellin integrals in (5) can be performed extremely fast. In fact, the calculation of $d\Delta\sigma$ becomes well over two orders of magnitude faster than for the “direct” method of computing it via Eq. (3). This brings one to the kinds of computational speeds needed for a full inclusion of pp scattering data in a NLO fitting analysis without having to resort to approximations. We note that the calculation of the arrays just mentioned is a major computational challenge; however, we found that this procedure can be made very efficient and fast by using adaptive Monte-Carlo sampling techniques.

Another crucial issue to be addressed in a global analysis is the estimate of the uncertainties in the extraction of the various Δf_j , associated with either experimental or theoretical uncertainties. We pursue here an approach based on the use of “Lagrange multipliers” (LM) [8, 11]. It has the advantage that no assumptions regarding, e.g., a quadratic behavior of the χ^2 function around the minimum need to be made. Rather, one investigates how χ^2 varies as a function of a particular observable or variable of interest. The uncertainty range is then defined by the region for which the increase $\Delta\chi^2$ in χ^2 above its lowest value is tolerable. In this way, one finds the largest possible range for predictions of a certain physical quantity that is consistent with a given $\Delta\chi^2$. Use of the LM method requires performing a huge number of fits, for which the efficiency of our Mellin method is crucial.

Results of global analysis.—We now present results for our NLO global analysis of DIS, SIDIS, and (in part preliminary) RHIC data. The data sets we take into account [2, 4] are listed in Tab. I together with their respective χ^2 values [12]. Notice that we use new sets of fragmentation functions (FFs) from Ref. [13], which are consistent with all relevant unpolarized SIDIS and RHIC data entering the spin asymmetries analyzed here. Uncertainty estimates of the FFs [13] are propagated in the computation of A_{LL} and included in χ^2 as a theoretical error. We use the strong coupling α_s and unpolarized PDFs of Ref. [14]. Other sets [15] give very similar results.

Rather than imposing the standard SU(2) and SU(3) symmetry constraints on the first moments of the quark and antiquark distributions, we allow for deviations:

$$\Delta\mathcal{U} - \Delta\mathcal{D} = (F + D)[1 + \varepsilon_{\text{SU}(2)}], \quad (6)$$

$$\Delta\mathcal{U} + \Delta\mathcal{D} - 2\Delta\mathcal{S} = (3F - D)[1 + \varepsilon_{\text{SU}(3)}], \quad (7)$$

where $\Delta\mathcal{F} \equiv [\Delta f_j^1 + \Delta \bar{f}_j^1](Q_0^2)$, $F + D = 1.269 \pm 0.003$, $3F - D = 0.586 \pm 0.031$ [2], and $\varepsilon_{\text{SU}(2,3)}$ are free parameters. In total we have fitted 26 parameters [16], setting $\gamma_{\bar{u}, \bar{d}, \bar{s}, g} = 0$ in Eq. (4). Positivity relative to the unpolarized PDFs of Ref. [14] is enforced at Q_0 . In Fig. 1 we compare the results of our fit using $Q = p_T$ to RHIC data from polarized pp collisions at 200 GeV [4], included for the first time in a NLO global fit. The bands are obtained with the LM method applied to each data point and correspond to the maximum variations for A_{LL} com-

TABLE I: Data used in our analysis [2, 4], the individual χ^2 values, and the total χ^2 of the fit. We employ cuts of $Q, p_T > 1$ GeV for the DIS, SIDIS, and RHIC high- p_T data.

experiment	data	data points	χ^2
	type	fitted	
EMC, SMC	DIS	34	25.7
COMPASS	DIS	15	8.1
E142, E143, E154, E155	DIS	123	109.9
HERMES	DIS	39	33.6
HALL-A	DIS	3	0.2
CLAS	DIS	20	8.5
SMC	SIDIS, h^\pm	48	50.7
HERMES	SIDIS, h^\pm	54	38.8
	SIDIS, π^\pm	36	43.4
	SIDIS, K^\pm	27	15.4
COMPASS	SIDIS, h^\pm	24	18.2
PHENIX (in part prel.)	200 GeV pp, π^0	20	21.3
PHENIX (prel.)	62 GeV pp, π^0	5	3.1
STAR (in part prel.)	200 GeV pp, jet	19	15.7
TOTAL:		467	392.6

puted with alternative fits consistent with an increase of $\Delta\chi^2 = 1$ or $\Delta\chi^2/\chi^2 = 2\%$ in the total χ^2 of the fit.

Our newly obtained antiquark and gluon PDFs are shown in Fig. 2 and compared to previous analyses [6, 8]. For brevity, the total $\Delta u + \Delta \bar{u}$ and $\Delta d + \Delta \bar{d}$ densities are not shown as they are very close to those in all other fits [6, 7, 8]. Here, the bands correspond to fits which maximize the variations of the truncated first moments,

$$\Delta f_j^{1,[x_{\min}-x_{\max}]}(Q^2) \equiv \int_{x_{\min}}^{x_{\max}} \Delta f_j(x, Q^2) dx, \quad (8)$$

at $Q^2 = 10 \text{ GeV}^2$ and for $[0.001 - 1]$. As in Ref. [8] they can be taken as faithful estimates of the typical uncertainties for the antiquark densities. For the elusive polarized gluon distribution, however, we perform a more detailed estimate, now discriminating three regions in x : $[0.001 - 0.05]$, $[0.05 - 0.2]$ (roughly corresponding to the range probed by RHIC data), and $[0.2 - 1.0]$. Within each region, we scan again for alternative fits that maximize the variations of the truncated moments $\Delta g^{1,[x_{\min}-x_{\max}]}$, sharing evenly to $\Delta\chi^2$. In this way we can produce a larger variety of fits than for a single $[0.001 - 1]$ moment, and, therefore, a more conservative estimate. Such a procedure is not necessary for antiquarks whose x -shape is already much better determined by DIS and SIDIS data. One can first of all see in Fig. 2 that $\Delta g(x, Q^2)$ comes out rather small, even when compared to fits with a “moderate” gluon polarization [6, 8], with a possible node in the distribution. This is driven mainly by the RHIC data, which put a strong constraint on the size of Δg for $0.05 \lesssim x \lesssim 0.2$ but cannot determine its sign as they

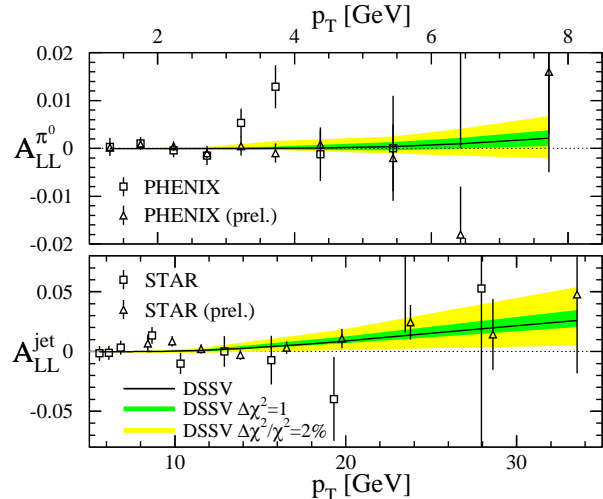


FIG. 1: Comparison of RHIC data [4] and our fit. The shaded bands correspond to $\Delta\chi^2 = 1$ and $\Delta\chi^2/\chi^2 = 2\%$ (see text).

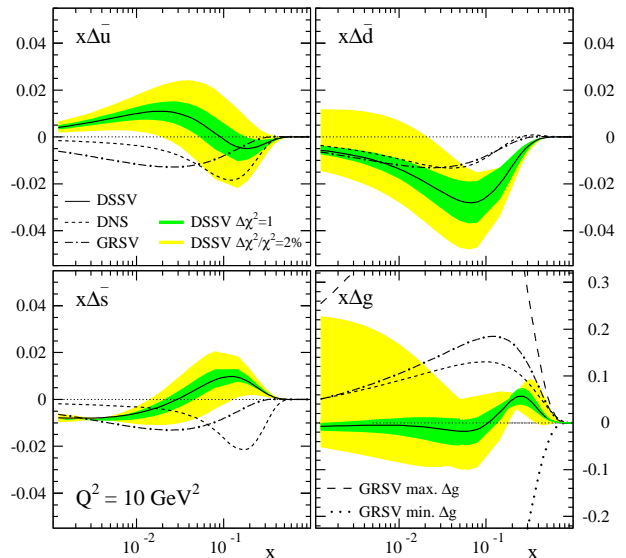


FIG. 2: Our polarized sea and gluon densities compared to previous fits [6, 8]. The shaded bands correspond to alternative fits with $\Delta\chi^2 = 1$ and $\Delta\chi^2/\chi^2 = 2\%$ (see text).

mainly probe Δg squared. To explore this further, Fig. 3 shows the χ^2 profile and partial contributions $\Delta\chi_i^2$ of the individual data sets for variations of $\Delta g^{1,[0.05-0.2]}$. A nice synergy of the different data sets is found. A small Δg at $x \simeq 0.2$ is also consistent with data from lepton-nucleon scattering [5], which still lack a proper NLO description. The small x region remains still largely unconstrained, making statements about Δg^1 not yet possible.

We also find that the SIDIS data give rise to a robust pattern for the sea polarizations, clearly deviating from SU(3) symmetry, which awaits further clarification from

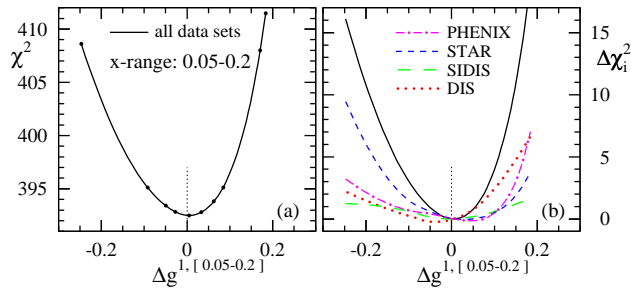


FIG. 3: The χ^2 profile (a) and partial contributions $\Delta\chi_i^2$ (b) of the data sets for variations of $\Delta g^{1,[0.05-0.2]}$ at $Q^2 = 10 \text{ GeV}^2$.

TABLE II: First moments $\Delta f_j^{1,[x_{\min}^{-1}]}$ at $Q^2 = 10 \text{ GeV}^2$.

	$x_{\min} = 0$	$x_{\min} = 0.001$	
	best fit	$\Delta\chi^2 = 1$	$\Delta\chi^2/\chi^2 = 2\%$
$\Delta u + \Delta \bar{u}$	0.813	0.793 ^{+0.011} _{-0.012}	0.793 ^{+0.028} _{-0.034}
$\Delta d + \Delta \bar{d}$	-0.458	-0.416 ^{+0.011} _{-0.009}	-0.416 ^{+0.035} _{-0.025}
$\Delta \bar{u}$	0.036	0.028 ^{+0.021} _{-0.020}	0.028 ^{+0.059} _{-0.059}
$\Delta \bar{d}$	-0.115	-0.089 ^{+0.029} _{-0.029}	-0.089 ^{+0.090} _{-0.080}
$\Delta \bar{s}$	-0.057	-0.006 ^{+0.010} _{-0.012}	-0.006 ^{+0.028} _{-0.031}
Δg	-0.084	0.013 ^{+0.106} _{-0.120}	0.013 ^{+0.702} _{-0.314}
$\Delta \Sigma$	0.242	0.366 ^{+0.015} _{-0.018}	0.366 ^{+0.042} _{-0.062}

the upcoming W boson program at RHIC. A particularly interesting result emerges for the polarized strange quark distribution: a fit that excludes the SIDIS data prefers a negative Δs , but with SIDIS data included, Δs is forced to be positive for $x \gtrsim 0.02$, in agreement with a recent LO analysis in [3]. From the fit we find breaking parameters $\varepsilon_{\text{SU}(2,3)}$ in (6), (7) very close to zero, so that the first moment of Δs must be negative. Therefore, in the full fit, Δs turns negative at small x , gaining most of its area there. This is also visible in Tab. II, where we show the full and truncated first moments of our PDFs. The behavior of Δs also leaves its imprint on the quark singlet, $\Delta \Sigma$. Notice that below $x \simeq 0.001$, where no data are available, the contributions to the full moments are determined by extrapolation of the distributions rather than constrained by the fit.

Conclusions.—We have presented the first global NLO QCD analysis of DIS, SIDIS, and preliminary RHIC data in terms of the helicity parton distributions. A technique based on the use of Mellin moments of the PDFs allows to efficiently incorporate the data from pp scattering at RHIC in a full and consistent NLO analysis. We have found that the RHIC data set significant constraints on the gluon helicity distribution, providing evidence that $\Delta g(x, Q^2)$ is small in the accessible range of momentum fraction. We also found that the SIDIS data clearly point

to a mostly positive $\Delta \bar{u}$ and a negative $\Delta \bar{d}$. The strange quark distribution Δs comes out negative at $x \lesssim 0.02$ and positive at higher x , even though here the systematic uncertainties inherent in SIDIS are arguably largest.

While our study should and will be improved on a number of aspects, in particular related to the inclusion of theoretical uncertainties and the treatment of experimental ones, we believe that it opens the door to finally obtaining a better and more reliable picture of the spin structure of the nucleon. In particular, it will help RHIC to realize its full potential, as hopefully more and more precise data will emerge over the next few years. We finally note that use of our fast and efficient Mellin technique for incorporating NLO pp scattering cross sections in the analysis is of course not restricted to RHIC, but could equally find important applications at the LHC.

We thank E.C. Aschenauer, A. Bazilevsky, A. Deshpande, R. Fatemi, S. Kuhn, and B. Surrow for communications. W.V. thanks the U.S. Department of Energy (contract no. DE-AC02-98CH10886). This work was partially supported by CONICET, ANPCyT and UBACyT.

- [1] See, e.g.: S. D. Bass, Rev. Mod. Phys. **77**, 1257 (2005).
- [2] See, e.g., [1] for a review of available data. Recent results can be found in: K.V. Dharmawardane *et al.*, Phys. Lett. **B641**, 11 (2006); A. Airapetian *et al.*, Phys. Rev. **D75**, 012007 (2007); *ibid.* **D76**, 039901 (2007)(E); V.Yu. Alexakhin *et al.*, Phys. Lett. **B647**, 8 (2007); M. Alekseev *et al.*, Phys. Lett. **B660**, 458 (2008).
- [3] A. Airapetian *et al.*, arXiv:0803.2993 [hep-ex].
- [4] A. Adare *et al.*, Phys. Rev. **D76**, 051106 (2007); K. Boyle, talk at the 2007 RHIC & AGS Users' Meeting, BNL, June 2007; B.I. Abelev *et al.*, arXiv:0710.2048 [hep-ex]; M. Sarsour, talk at the 2007 APS DNP meeting, Newport News, Virginia, Oct. 2007.
- [5] P. Liebing, AIP Conf. Proc. **915**, 331 (2007); E.S. Ageev *et al.*, Phys. Lett. **B633**, 25 (2006).
- [6] M. Glück *et al.*, Phys. Rev. **D63**, 094005 (2001).
- [7] J. Blümlein and H. Böttcher, Nucl. Phys. **A721**, 333 (2003); E. Leader *et al.*, Phys. Rev. **D73**, 034023 (2006); M. Hirai *et al.*, Phys. Rev. **D74**, 014015 (2006).
- [8] D. de Florian *et al.*, Phys. Rev. **D71**, 094018 (2005); G.A. Navarro and R. Sassot, Phys. Rev. **D74**, 011502 (2006).
- [9] M. Stratmann and W. Vogelsang, Phys. Rev. **D64**, 114007 (2001).
- [10] D. de Florian, Phys. Rev. **D67**, 054004 (2003); B. Jäger *et al.*, Phys. Rev. **D67**, 054005 (2003); **D70**, 034010 (2004).
- [11] D. Stump *et al.*, Phys. Rev. **D65**, 014012 (2002).
- [12] We add statistical and systematical errors in quadrature as full error correlation matrices are not always available.
- [13] D. de Florian *et al.*, Phys. Rev. **D75**, 114010 (2007); **D76**, 074033 (2007).
- [14] A.D. Martin *et al.*, Eur. Phys. J. **C28**, 455 (2003).
- [15] J. Pumplin *et al.*, JHEP **0207**, 012 (2002).
- [16] A FORTRAN code, list of fitted parameters, and additional material can be found at ribf.riken.jp/~marco/DSSV.